Biomed Microdevices (2016) 18:95
DOI 10.1007/s10544-016-0120-9

Autoinducer-2 analogs and electric fields - an antibiotic-free bacterial biofilm combination treatment

Sowmya Subramanian [1,2] · Konstantinos Gerasopoulos [1] · Min Guo [3] · Herman O. Sintim [3] · William E. Bentley [4,5] · Reza Ghodssi [1,2,4]

Abstract Bacterial biofilms are a common cause of chronic medical implant infections. Treatment and eradication of biofilms by conventional antibiotic therapy has major drawbacks including toxicity and side effects associated with high-dosage antibiotics. Additionally, administration of high doses of antibiotics may facilitate the emergence of antibiotic resistant bacteria. Thus, there is an urgent need for the development of treatments that are not based on conventional antibiotic therapies. Presented herein is a novel bacterial biofilm combination treatment independent of traditional antibiotics, by using low electric fields in combination with small molecule inhibitors of bacterial quorum sensing – autoinducer-2 analogs. We investigate the effect of this treatment on mature *Escherichia coli* biofilms by application of an alternating and offset electric potential in combination with the small molecule inhibitor for 24 h using both macro and micro-scale devices. Crystal violet staining of the macro-scale biofilms shows a 46 % decrease in biomass compared to the untreated control. We demonstrate enhanced treatment efficacy of the combination therapy using a high-throughput polydimethylsiloxane-based microfluidic biofilm analysis platform. This microfluidic flow cell is designed to reduce the growth variance of *in vitro* biofilms while providing an integrated control, and thus allows for a more reliable comparison and evaluation of new biofilm treatments on a single device. We utilize linear array charge-coupled devices to perform real-time tracking of biomass by monitoring changes in optical density. End-point confocal microscopy measurements of biofilms treated with the autoinducer analog and electric fields in the microfluidic device show a 78 % decrease in average biofilm thickness in comparison to the negative controls and demonstrate good correlation with real-time optical density measurements. Additionally, the combination treatment showed 76 % better treatment efficacy compared to conventional antibiotic therapy. Taken together these results suggest that the antibiotic-free combination treatment described here may provide an effective alternative to traditional antibiotic therapies against bacterial biofilm infections. Use of this combination treatment in the medical and environmental fields would alleviate side effects associated with high-dosage antibiotic therapies, and reduce the rise of antibiotic-resistant bacteria.

Keywords Autoinducer analogs · Quorum sensing · Biofilms · Bioelectric effect · Polydimethylsiloxane · Microfluidics · Micro-systems

Electronic supplementary material The online version of this article (doi:10.1007/s10544-016-0120-9) contains supplementary material, which is available to authorized users.

✉ Sowmya Subramanian
dr.sowmya.subramanian@gmail.com

✉ Reza Ghodssi
ghodssi@umd.edu

[1] MEMS Sensors and Actuators Laboratory, Institute for Systems Research, University of Maryland, 2201 J.M. Patterson Building, College Park, MD 20742, USA

[2] Department of Electrical and Computer Engineering, University of Maryland, 2435 A.V. Williams Building, College Park, MD 20742, USA

[3] Department of Chemistry and Biochemistry, University of Maryland, 0107 Chemistry Building, College Park, MD 20742, USA

[4] Fischell Department of Bioengineering, University of Maryland, 2330 Jeong H. Kim Engineering Building, College Park, MD 20742, USA

[5] Department of Chemical and Biomolecular Engineering, University of Maryland, 2113 Chemical & Nuclear Engineering Building, College Park, MD 20742, USA

Published online: 19 September 2016

1 Introduction

Bacterial biofilms are complex communities comprised of extra-cellular matrix (ECM) and bacteria. These biofilms are the primary cause of infections in medical implants and catheters, and are also a major contaminant of the environment that leads to disease transmission (Costerton et al. 1999; Ghannoum and O'Toole 2004; Huq et al. 2008). Bacteria in biofilms are known to exchange genes including those responsible for antibiotic resistance. Additionally, the ECM hinders diffusion of the antibiotic treatments, resulting in much higher resistance than planktonic bacteria. This necessitates the use of very high doses of conventional antibiotics for eradication of biofilms (from 500 to 5000 times the minimum inhibitory concentration (MIC)) in comparison to planktonic bacteria (Characklis 1981; Costerton et al. 1999; Stoodley et al. 2002; Fux et al. 2003; Ghannoum and O'Toole 2004; Al-Nasiry et al. 2007; Pozo and Patel 2007). Such high antibiotic concentrations are practically impossible to achieve using conventional antibiotic therapies due to the associated toxicities and side effects and the limitation of renal and hepatic functions. The use of high doses of antibiotics to treat biofilms and bacteria in general, also leads to the emergence of antibiotic-resistant bacterial strains (Anderson and O'toole 2008), thereby necessitating the development of alternative methods of treatment that are not based on traditional antibiotic therapy.

While antibiotics are established treatments for bacterial infections, autoinducer-2 (AI-2) analogs have recently been shown to inhibit biofilms by preventing bacterial communication or quorum sensing (QS) that is critical to biofilm formation (Roy et al. 2009, 2010, 2011). QS is a key process used by bacteria in colonies to communicate with each other, collectively actuate gene expression and establish recalcitrant biofilms. QS is a molecular signaling system by which bacteria synthesize, uptake, and actuate gene expression. It is mediated by small molecules known as autoinducers (AI). Autoinducer-2 (AI-2) is a class of small molecules produced by a variety of species of bacteria that mediate communication among various bacteria, including those of disparate genetic history (Miller and Bassler 2001; Waters and Bassler 2005; Quan and Bentley 2012). Analogs of the AI-2 molecules work through the native signal transduction pathway and block signaling, inhibiting QS. That is, AI-2 analog molecules, upon uptake by the bacteria, bind to and prevent transcription of genes crucial to QS, thereby inhibiting or reducing biofilm formation (Roy et al. 2010, 2011; Gamby et al. 2012). Synthetic AI-2 analogs can be engineered to target different species of bacteria by changing the alkyl group attached to C1 carbon (Roy et al. 2010). Thus, AI-2 analogs show promise as a new class of anti-biofilm agents that is different from traditional antibiotic therapies (Roy et al. 2013). It has been suggested that since analog molecules do not directly kill the bacteria, but only inhibit QS or virulent states of the bacteria like biofilms, the probability of resistance development to small molecule inhibitors is significantly reduced (Rasmussen and Givskov 2006a, b; Roy et al. 2011). Furthermore, initial studies of these analog molecules suggest no visible toxic side effects on epithelial cell lines making AI-2 analogs a prime candidate for biofilm treatment.

In previous work, we demonstrated that these analogs could be used to increase the efficacy of traditional antibiotic treatment, specifically with gentamicin. When combined with minimum inhibitory concentration (MIC) levels of antibiotics, the combination treatment was significantly more efficient in removing pre-existing mature biofilms than either antibiotic or analog treatment by itself (Roy et al. 2013). Another promising method to increase the efficacy of antibiotics on biofilms is a combinatorial treatment based on simultaneous application of electrical signals with antibiotics at low or near MIC doses. The treatment of biofilms using a combination of electric fields and MIC levels of antibiotics has been referred to as bioelectric effect (BE) (Costerton et al. 1994; Wellman et al. 1996; Stoodley et al. 1997). We have demonstrated that at voltages below those needed for electrolysis of water, the energy of the electrical signal plays a crucial role in determining the efficacy of the BE treatment (Kim et al. 2015). Although the exact mechanism of action is still unknown and various theories exist, one of the primary hypotheses is that the observed increase in efficacy is due to the increased permeation of the antibiotic into the ECM of the biofilm due to the electric field application (Pareilleux and Sicard 1970; Blenkinsopp et al. 1992; Wellman et al. 1996). In this work, we hypothesize that combining AI-2 analog small molecule inhibitors with electric fields similarly enables more efficient and effective permeation of the analog molecule into the biofilm. We envision that such increased analog concentration within the biofilm results in a significantly higher reduction in biofilm as compared to individual analog treatments, while eliminating reliance on antibiotics.

In this work, we seek to improve the established treatment efficacy of QS analogs by combining it with electric fields. We evaluate the efficacy of this antibiotic-free combinational treatment using *Escherichia coli* biofilms as the model organism and compare the results of the treatment with control, analog-only and electric field-only therapies when applied to uniform biofilms. We note the experimental evaluation of such new treatment techniques is strongly hindered by the stochastic nature of biofilm growth (Roy et al. 2013; Meyer et al. 2015). Our previous experiments show that bacterial biofilms grown in single channel microfluidics exhibit a growth variation of ~75 % (Meyer et al. 2015). Therefore, a second and equally important component of our work is the development of a platform that facilitates multi-experiment

studies on uniform biofilms in parallel, where statistical validation can be confirmed. This is achieved with bifurcation microfluidics, which have distinct advantages in ease of fabrication over previous valve-based approaches (Meyer et al. 2015). The integration of linear array charge-coupled devices (CCDs) in the micro-scale system enables evaluation of new treatment in real-time (Kim et al. 2012; Subramanian et al. 2014, 2015; Kim et al. 2016). The CCD-based biofilm-monitoring platform was previously used and validated for single microfluidic channels (Kim et al. 2012, 2016). It is used in the current work as a means of validating the reduced growth variation of the bifurcation-based microfluidics. Such reduction in growth variance significantly improves experimental reliability when the platform is used as a test-bed for new treatment evaluation.

The ability of the microfluidic bifurcation device to serve as a reliable platform for biofilm studies is evaluated through both biofilm growth and treatment experiments. Specifically, the uniformity of mature biofilms grown in the microfluidic bifurcation device is verified using end-point confocal microscopy. The multi-experiment treatment application to the bifurcation channels is achieved through reversal of direction of flow. This experimental parameter (flow direction) never needed to be changed between growth and treatment phases in previous devices. Thus, the reliability of the bifurcation platform to perform parallel studies on uniform biofilms under reversal of direction of flow is established by demonstrating a previously proven combination treatment of AI-2 analogs and antibiotics. These experiments confirm the reduced biofilm thickness variation between the channels of the device during biofilm growth and the reliability of this platform to test multiple treatments in parallel.

For the first time, both macro-scale static biofilms and microfluidic dynamic biofilms were subjected to the novel antibiotic-free combination therapy and shown to result in a significant decrease in biomass. Multiple measurement techniques, CV staining and confocal microscopy results, are offered and compared to the real-time OD measurements in this work. CV staining of the macro-scale static biofilms showed a 46 % decrease in biomass when treated using the combination therapy in comparison to the untreated control. Confocal microscopy measurements of the dynamic biofilms treated with the AI-2 analog and electric fields in the microfluidic flow cell resulted in a 78 % decrease in biofilm thickness in comparison to the controls. Furthermore, the average real-time OD measurements obtained using the CCD platform correlated well with end-point confocal measurements, in addition to the intrinsic benefits in terms of simplicity and accessibility. These results show that the combination of AI-2 analogs and electric fields can be used to treat mature and nascent biofilms. We envision this antibiotic-free method for treatment of biofilms will find utility in both clinical and environmental settings.

2 Materials and methods

2.1 Experimental design

2.1.1 Cuvette test apparatus

The macro-scale apparatus was designed to ensure uniform electric fields, while retaining access for sensing and fluid manipulation (Kim et al. 2015). Electroporation cuvettes (P460–50, Invitrogen Inc.) with parallel stainless steel electrodes forming two of the walls (0.4 cm gap between electrodes) were used to apply a near uniform electric field inside the cuvette (Fig. 1). A 500 μm thick Borofloat 33 wafer was diced into chips (or coupons) with dimensions of 0.8 cm × 4 cm (width × length). The diced glass chip was inserted upright into the cuvette between the two electrodes as shown in Fig. 1b and served as a consistent area for biofilm growth. The electrical signal was provided by a function generator (33,220 A, Agilent Inc.) with a coaxial cable connection to the electrical contact board.

2.1.2 Microfluidic device design

The microfluidic design is based on the principle of bifurcation with the final dimensions of each channels measuring 2 cm × 1 mm × 100 μm (length × width × depth). The microfluidic bifurcation-based method of controlling suspended particles and flow is primarily dependent on the design of the channel (Roberts and Olbricht 2006). In this work, the channels were designed with equal fluidic resistance at each bifurcation (angle of bifurcation =45° and equal channel dimensions and flow rates), to guarantee equal conditions in all daughter channels. This approach is more amenable to scale-up as compared to other methods of controlling particle flow such as changing local flow rates or pressures, or the use of microfluidic valves (Subramanian et al. 2014; Meyer et al. 2015). Figure 2 shows the schematic of a simple 2-level device that bifurcates into 4 daughter channels. This system allows for streamlined parallel experiments to be performed on a single biofilm grown in the same device under uniform growth conditions using a microfluidic design that only requires easy one step fabrication, thereby avoiding the need for complex structures like microfluidic valves.

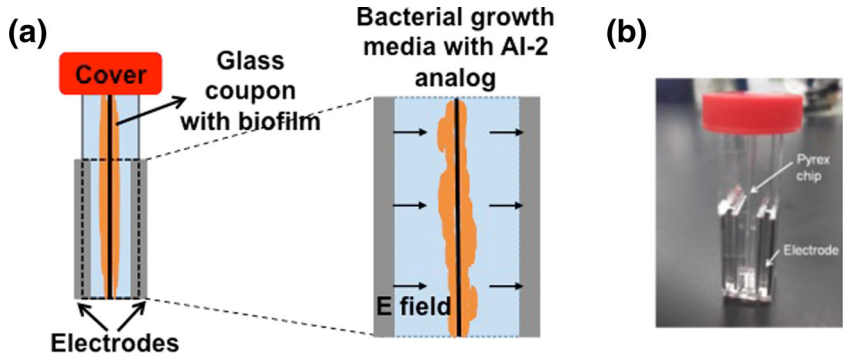

Fig. 1 **a** Schematic of the macro-scale experimental setup. **b** Photograph of electroporation cuvette with glass chip/coupon placed inside it

2.1.3 Microfluidic device experiments

We have partitioned experiments in two operating modes: a growth mode, where cells were introduced and biofilms are established and a treatment mode where small molecule inhibitor is added. During the growth mode, the bacterial suspension and the media were introduced from a common source and the flow is directed from the single common inlet to the 4 outlets as shown in Fig. 2a. Since the biofilms were grown simultaneously on the same device and from the same source of bacterial suspension, the variability between the biofilms grown in different channels was expected to be significantly lower than the variability of biofilms grown in separate single channels on separate devices. After establishment of biofilms, multiple treatments can be tested on the same device. During treatment, the direction of flow was reversed and different treatments were introduced through each channel of the device from the ports on the right-hand side, as shown in Fig. 2b. By introducing pure growth media in one of the channels (control), we ensured that results of the various treatment experiments performed on the same device were compared to a common control. For treatment testing, the AI-2 analog molecule specific to *E. coli* W3110 – iso-butyl DPD ((S)-4,5-dihydroxy-2,3-pentanedione) – was diluted in growth media to a final concentration of 100 μM. Thus, the treatment solutions introduced into the channels of the device were either pure Luria broth (LB) growth media (negative control and electric field-only) or the analog suspended in LB media (AI-2 analog-only and combination treatment).

2.1.4 Microfluidic device fabrication

We fabricated the microfluidic device using well-established soft lithography techniques. The mold was fabricated by patterning a 100 μm tall KMPR-1050 layer on a silicon substrate. The mold can be reused to produce multiple devices. PDMS (Sylgard 184, Dow Corning) in the ratio of 10:1 silicone elastomer to curing agent is poured over the mold and cured at 60 °C for 15 min. The PDMS was peeled off the mold and the inlet ports were punched using a 2 mm dermatological punch. The final device was irreversibly plasma bonded to a glass coverslip that was patterned with 20/200 nm of Cr/Au for application of electric fields (Fig. 3a). Tygon tubing was connected to the inlets and outlets of the device using a tubing coupler, and the other end of the tubing was connected to a syringe pump (KDS-230, KD Scientific) to enable fluid flow.

2.1.5 Electric field intensity

The electric field intensity used for treatment of *E. coli* biofilms was chosen such that no bulk electrolysis of the media occurs. Experiments previously performed on *E. coli* biofilms in LB determined that AC and DC electric fields less than 1.25 V/cm can be used without inducing bulk electrolysis of the media (Kim et al. 2015). The electrical potential used in this work was 0.125 V AC at 10 MHz offset by 0.125 V DC, significantly lower than the bulk hydrolysis potential of 0.82 V. This corresponds

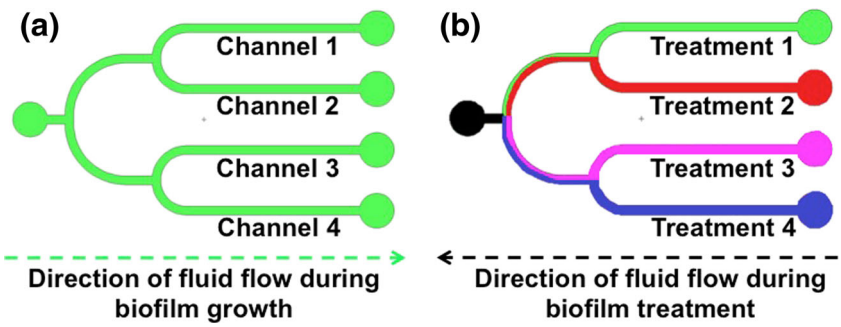

Fig. 2 Schematic of a 2-level bifurcation device with 4 daughter channels under different modes of operation. **a** Device during the biofilm growth phase. **b** Device during the biofilm treatment phase

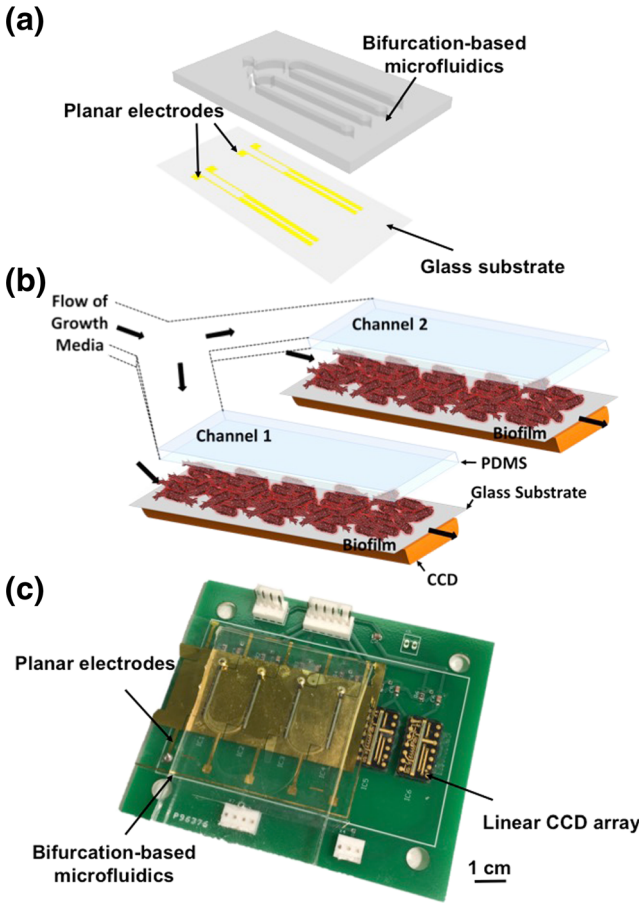

Fig. 3 **a** Schematic of the bifurcation-based microfluidic device. **b** Schematic of device integrated with the CCD monitoring platform. **c** Photograph of the CCD-based microfluidic system (scale bar = 1 cm)

to an electric field of 1.25 V/cm DC field with a 1.25 V/cm AC field at 10 MHz. The frequency of the AC electric field (10 MHz) was chosen based on previous work that was shown to be effective (Caubet et al. 2004; Giladi et al. 2010).

2.2 Biofilm growth

A bacterial suspension was prepared from *E. coli* K-12 W3110 samples(Wang et al. 2005) previously stored at −80 °C by inoculating in 5 mL of fresh LB. The suspension was cultured at 37 °C in a 250 rpm shaker for 18 h. The culture was reinoculated into fresh LB to achieve optical densities (OD_{600}) in the range of 0.20–0.25.

2.2.1 Cuvette test setup

1 mL of the reinoculated culture was placed in each cuvette with a glass coupon for 24 h of biofilm growth. *E. coli* biofilms formed on the chips over 24 h in LB medium at 37 °C (Stoodley et al. 1997; Stewart et al. 1999; Jun et al. 2010). The glass chips with pre-formed 24-h *E. coli* biofilms were transferred to a new set of cuvettes containing 1 mL of either LB only (control and electric field only) or 100 μM of isobutyl DPD, the AI-2 analog specific to *E. coli*, in LB (AI-2 analog and combination treatment) (Roy et al. 2010, 2013). Electric fields were applied for 24 h to the biofilm-containing cuvettes (no electric field was applied to the control or AI-2 analog only cuvettes). The biofilms were evaluated by performing crystal violet staining for total biomass quantification.

2.2.2 Microfluidic test setup

The reinoculated culture was introduced into the microfluidic device in growth mode at a flow rate of 100 μl/min using a syringe pump set in withdrawal mode. The suspension was allowed to seed (no flow) for 2 h to allow for attachment of bacteria to the glass substrate of the device. Subsequently, LB medium was introduced into each channel of the device at a flow rate of 20 μl/h per channel. After 24 h of biofilm growth, the direction of flow was reversed (syringe pump operated in infusion mode while accounting for the time the bacterial suspension in the tubing takes to flow back in through the device channels) and 100 μM of isobutyl DPD in LB (AI-2 analog and combination treatment channels) or pure LB (control and electric field only channels) were introduced into the channels at a flow rate of 20 μl/h per channel. The flow rates and time periods of the various experimental phases used in this work have been characterized previously (Meyer et al. 2011; Kim et al. 2012; Kim et al. 2016). The electrical signal was provided using a function generator (33,220 A, Agilent Inc.) with a coaxial cable connection to a spring-loaded pin that contacted the contact pad patterned on the device. While clinical biofilm growth may occur over long time periods like weeks or sometimes even months, for the purposes of the present study we chose biofilm growth and treatment periods of only 24 h each in order to reliably compare the antibiotic-free treatment results with other previously published treatment results (Kim et al. 2012, 2016). After specified times, the biofilms were stained as described section below (Roy et al. 2013). The stained biofilms were imaged using confocal microscopy to obtain biofilm thickness quantification and other characteristics.

2.3 Biofilm analysis

2.3.1 Crystal violet staining

The biofilms grown and treated in the macro-scale cuvette setup were quantified using the crystal violet (CV) staining method as previously described (Kim et al. 2015). After the

24 h biofilm growth followed by a 24 h biofilm treatment, the glass coupons were removed from each cuvette and gently rinsed with deionized (DI) water to remove non-adherent bacteria. The total biomass of the biofilm on the coupon was quantified by staining each coupon for 15 min using 0.1 % CV stain (O'Toole et al. 1999; Merritt et al. 2005). Following this, each coupon was gently immersed and rinsed sequentially in 4 prepared beakers of clean DI water to remove any unbound crystal violet. After the coupons were rinsed in DI water, the stained biofilms were resuspended in 1.5 mL decomplexation solution of 80 % ethanol and 20 % acetone for 30 min (O'Toole et al. 1999; Merritt et al. 2005). The optical density at 540 nm (OD_{540}) of the decomplexation solution was measured using a spectrophotometer (Spectramax Plus, Molecular Devices). The final OD_{540} of the crystal violet released from the biofilms is proportional to the total biomass growth on the coupon.

2.3.2 Real-time biofilm monitoring

We have previously demonstrated optical density monitoring of biofilms using CCDs (Kim et al. 2012; Subramanian et al. 2014). In this work, the CCDs (TSL1402R, Texas Advanced Optoelectronic Solutions) feature 128 × 1 linear pixel arrays with individual photodiodes measuring 120 μm (H) by 71.5 μm (W) spaced 55.5 μm apart, thereby spanning an overall array length of 1.6 cm. A schematic and photograph of the platform are shown in Fig. 3c-d. An external diffusive edge-lit LED light panel (Luminous Film) was used to illuminate the platform uniformly. The wavelength of the light source was 630 nm in order to match the sensitivity of the CCDs. The CCDs were driven by an external power supply (E3631A, Agilent Technologies), and function generators (33,220 A, Agilent Technologies) and were used to control the data sampling. The signal readout from the device was achieved using a data acquisition card (NI USB-6221, National Instruments) programed to record data using LabView.

2.3.3 Confocal microscopy

Biofilms grown in the microfluidic device were stained, imaged and analyzed using protocols described previously (Meyer et al. 2011; Roy et al. 2013). After biofilm growth and treatment the biofilms were stained with Filmtracer™ LIVE/DEAD® Biofilm Viability Kit (Molecular Probes, Inc.), using a mixture of 10 μl each of the SYTO9 and propidium iodide stains introduced at a flow rate of 20 μl/h per channel. This was followed with treatment with a 100 μg/mL solution of calcofluor (Fluorescence Brightner 28, Sigma #F2543), which stains the beta-linked polysaccharides contained in the biofilm matrix (Roy et al. 2013). The biofilms were then imaged using confocal microscopy (LSM 710, Zeiss). Three spots in the channels of the bifurcation device were imaged: one near the inlet, the second near the center and the third near the outlet of the channel. The Z-stacks obtained were analyzed using the software package COMSTAT(Heydorn et al. 2000) and visualized using Imaris (Bitplane Inc.).

3 Results and discussion

3.1 Cuvette test setup

Initial testing of the combination treatment was performed using the macro-scale setup as it facilitated rapid treatment assessment using commercially available electroporation cuvettes. It also enabled application of uniform electric fields across the biofilm on the glass coupon, while providing access for fluid handling. To test and compare the efficacy of the combination treatment of AI-2 analog (isobutyl DPD) and electric fields, 24-h mature *E. coli* biofilms were subjected to four different treatments for an additional 24 h, viz. (1) control, (2) AI-2 analog, (3) electric fields only, and (4) combination of AI-2 analog and electric fields. The biofilms were then quantified using the CV staining method and the results of this experiment are shown in Fig. 4.

Clearly, in this static biofilm setup, application of only electric fields resulted in no apparent reduction in total biomass and treatment with 100 μM AI-2 analog, isobutyl DPD yielded a negligible decrease in total biomass (ANOVA $p = 0.46$) in comparison to the untreated controls. This is comparable to the results obtained when 24-h *E. coli* W3110

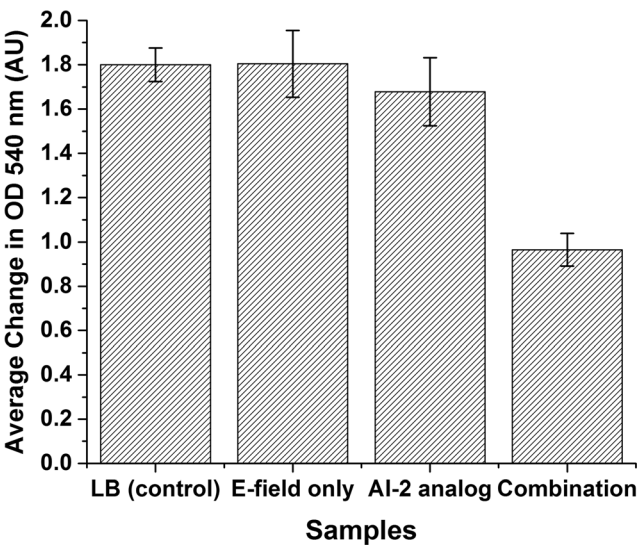

Fig. 4 Plot showing efficacy of new combination treatment that is independent of antibiotics using the macro-scale cuvette setup. Treatment with the combination therapy results in a 46.4 ± 4.1 % decrease in total biomass compared to the controls. The error bars represent the standard deviation across three samples ($n = 3$)

biofilms grown in a 96-well plate (static conditions) were treated with increasing concentrations (0 μM, 50 μM, 250 μM, and 500 μM) of isobutyl DPD (online supplemental reference Fig. S1). Colorimetric measurements of viable cells density and the ECM were performed using previously established protocols (Toté et al. 2008). Wild type biofilm forming *E. coli* W3110 (online supplemental reference Fig. S1a) and mutant strain *E. coli* MDAI2 that has diminished biofilm function (online supplemental reference Fig. S1b) treated with increasing concentrations of AI-2 analog (isobutyl DPD) showed no decrease in viable cell density (DeLisa et al. 2001; Meyer et al. 2011). In the wild type strain, it was observed that AI-2 analogs did not kill viable cells in the biofilm but aided in reducing ECM formation at analog concentrations of 500 μM. It is hypothesized that the slight reduction in viable cells on treatment with 500 μM AI-2 analog was due to reduced ECM upon which the bacterial cells may adhere to. The *E. coli* MDAI2 cells, when treated with increasing concentrations of the analog, showed no change in the viable cell count even at 500 μM, suggesting that the analog only helps reduce biofilm matrix formation and does not directly affect viable bacterial cells. These experiments performed in a static environment show that the AI-2 analog does not inhibit the growth of biofilms at concentrations of 100 μM. However, as shown in Fig. 4, treatment of biofilms with lower concentrations of isobutyl DPD in combination with electric fields resulted in a significant decrease in total biomass as compared to the untreated controls. These results demonstrate that the efficacy of the small molecule inhibitor can be increased dramatically, even at such low concentrations, through the application of a small electric field. Specifically, treatment with the combination therapy resulted in a 46.4 ± 4.1 % reduction compared to the untreated control and a 42.5 ± 4.4 % decrease in comparison to treatment with 100 μM of isobutyl DPD only (ANOVA $p = 0.0002$).

We suggest that the AI-2 analog treatment when combined with electric fields, enables permeation of the biofilm more rapidly, similar to the antibiotic molecule during application of the bioelectric effect. The increased permeation into the biofilm makes more AI-2 analog molecules available in the bulk of the biofilm. In turn the rise in concentration of AI-2 analog in the biofilm, increases the probability that isobutyl DPD is imported into cells, phosphorylated by the QS kinase, LsrK, and then binds to the cognate transcriptional regulator, LsrR (Roy et al. 2010), thereby acting as a QS antagonist, quenching QS activities (Waters and Bassler 2005) and preventing further production of proteins necessary for biofilm ECM production. Such reduced ECM production may decrease the structural strength and stability of the biofilm, resulting in easier removal of the biofilm due to the shear experienced in the microfluidic channel. It is hypothesized that the increased shear experienced in the microfluidic channel is a contributing factor in the higher treatment efficacy observed in the microfluidic flow cell as opposed to the macro-scale cuvette setup.

3.2 Microfluidic test setup

E. coli biofilms were grown in the channels of the bifurcation device for 24 h, and subsequently exposed to the four experimental conditions – control, electric fields only, AI-2 analog isobutyl DPD, and the combination of AI-2 analog and electric fields. The respective solutions were introduced into the four channels of the device over an additional 24 h. Both end point confocal microscopy images, and CCD-based real-time monitoring of biofilm growth and treatment were performed. These results are discussed below.

3.2.1 Uniform biofilm growth validation using end-point confocal microscopy

To validate the uniformity of biofilms in the channels, *E. coli* biofilms grown in three microfluidic devices over 72 h were imaged using confocal microscopy and analyzed using COMSTAT (Heydorn et al. 2000). Fresh LB media was introduced into the channels every 24 h. A longer duration of biofilm growth was chosen in order to verify if biofilm uniformity could be maintained over periods larger than 24 h.

Figure 5a plots the average biofilm thickness across the channels of the three bifurcation devices. The variance between biofilms grown in the same device was calculated to be 7.1 % as compared to the inter-device variability of 21 %. The reduction in intra-device biofilm thickness variation is comparable to that observed in the microfluidic biofilm segmentation device (Meyer et al. 2015), and highlights the potential limits in reduction of biofilm growth variation achievable in microfluidic systems. However, this reduced intra-device variance is significantly lower than the 75 % inter-device variation observed when using single channel microfluidic devices (Meyer et al. 2015), which enabled more reliable comparison of the various treatments applied to the biofilms grown on the same bifurcation device. By exposing one of the channels to LB only (no treatment), we ensured that the results of the various experiments performed on the same device are compared to a common control. Figure 5b-e present surface rendered confocal microscopy images from each channel. The colors in the image correspond to different components of the biofilm. The red represents dead cells, the green represents live cells and the blue represents the ECM of the biofilm.

3.2.2 Microfluidic treatment mode validation using end-point confocal microscopy

The reliability of using this platform as a test bed for biofilm treatment characterization and evaluation was

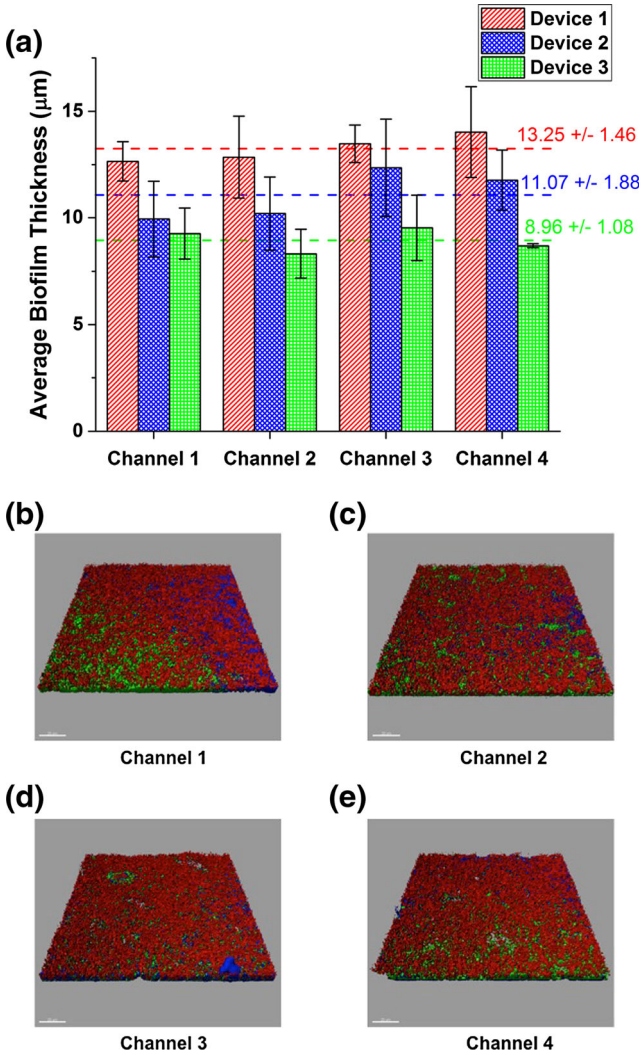

Fig. 5 **a** Plot showing uniformity of biofilms growth between the channels of the each device. The variability between the channels of each device is less than 10 %, whereas inter device variability is 21 %. The error bars represent the standard deviation across three confocal images (n = 3) obtained in each channel of the device. **b**-**e** Surface rendered sample confocal microscopy images from device 3 (scale bar =20 μm). The thicknesses were 10.61 μm (channel 1), 8.22 μm (channel 2), 8.21 μm (channel 3) and 8.75 μm (channel 4). The colors in the image correspond to different components of the biofilm. The green and red represents live and dead cells and the blue represents the ECM of the biofilm

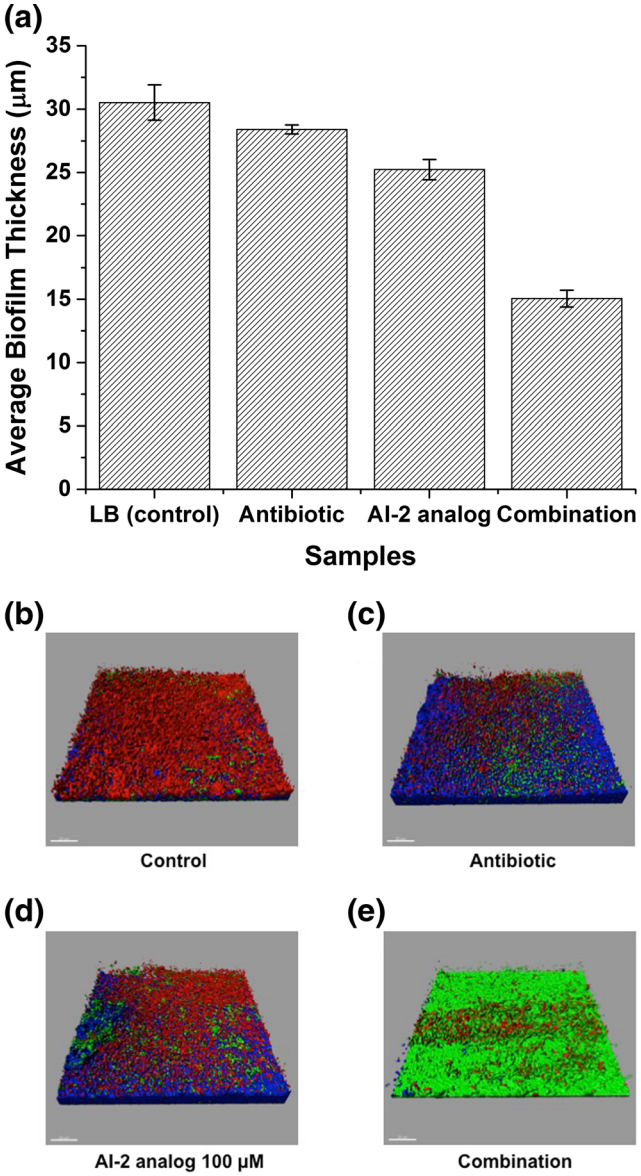

Fig. 6 Verification of biofilm treatment testing using the bifurcation device. **a** End-point confocal microscopy of the combination treatment of the antibiotic gentamicin and AI-2 analog as applied to 24-h E.coli W3110 biofilms resulted in a 50.7 ± 2.2 % decrease in biofilm thickness as compared to the control. This is similar to previously obtained results (Roy et al. 2013). The error bars represent the standard deviation across three confocal images ($n = 3$) obtained in each channel of the device. **b**-**e** Surface rendered sample confocal microscopy images from the device (scale bar =20 μm). The thicknesses were 29.57 μm (control), 28.62 μm (antibiotic), 26.08 μm (AI-2 analog) and 14.31 μm (combination). The colors in the image correspond to different components of the biofilm. The green and red represents live and dead cells and the blue represents the ECM of the biofilm

verified by analyzing biofilms subjected to previously reported therapies using the protocols listed above. Presented in Fig. 6 are the results of subjecting 24-h *E. coli* W3110 biofilms to an antibiotic (gentamicin, 10 μl/ml), AI-2 analog (isobutyl DPD, 100 μM), and the combination of AI-2 analogs and antibiotics. As observed, the antibiotic treatment resulted in minimal change compared to the control (ANOVA $p = 0.1$), as measured by biofilm thickness calculations using COMSTAT (Heydorn et al. 2000). Treatment with 100 μM isobutyl-DPD showed a slightly higher reduction of 17.4 ± 2.6 % with respect to the untreated control and antibiotic treatment (ANOVA $p = 0.0014$). However, treatment with the combination of near MIC levels gentamicin and 100 μM isobutyl DPD

significantly enhanced the treatment and resulted in a decrease of 50.7 ± 2.2 % (ANOVA $p < 0.0001$). Due to the inherent complex heterogeneous structure of biofilms, in which the live persister cells are surrounded by the dead cells and the ECM (Costerton et al. 1999), a significant reduction in biofilm thickness as a result of treatment with the combination of AI-2 analogs and antibiotics exposes the viable cells in the core of the biofilm. This appears as an increase in viable cells, as represented by the green color of the confocal image shown in Fig. 6e. These correlate with previously published results (Roy et al. 2013), thereby validating the use of this platform for treatment testing of biofilms.

3.2.3 Antibiotic-free combination treatment testing using end-point confocal microscopy

To test the efficacy of the antibiotic-free combination therapy (AI-2 analogs and electric fields), *E. coli* biofilms were grown in the bifurcation device for 24 h and exposed to the four treatments for an additional 24 h. The biofilms were then stained and imaged using confocal microscopy. Figure 7 plots the average thickness of the biofilm after treatment. As shown, application of only an electric field results in no significant decrease in biofilm thickness (ANOVA $p = 0.36$). Treatment with 100 μM AI-2 analog isobutyl DPD resulted in a 31.1 ± 10.1 % decrease in biofilm thickness as compared to the control (ANOVA $p = 0.023$). This correlates with data obtained using single channel microfluidics (online supplemental reference Fig. S2), consistent with previous work (Roy et al. 2013). Treatment with the combination therapy resulted in a significant decrease in biofilm as measured by the 77.8 ± 6.3 % (ANOVA $p = 0.0001$) decrease in average thickness as compared to the control. The larger percentage decrease in biomass following treatment using the microfluidic platform (77.8 %), in contrast to the cuvette test setup (46.4 %), is attributable to the flow in the microfluidic setup. Firstly, we suggest that the microfluidic flow ensures availability of fresh AI-2 analog molecules at the biofilm site. In contrast, the cuvette setup limits AI-2 analog availability at the biofilm surface to purely diffusion. Secondly, we postulate that the higher efficacy in the microfluidic device can also be attributed to the shear in the channel adding to the increased penetration of the treatment into the biofilm as well as to easier removal of the biofilm. We also note here that the biofilm thicknesses observed for the LB growth media only and the 100 μM AI-2 analog controls in Fig. 6 and Fig. 7 are significantly different despite similar experimental conditions. This inherent variability in biofilm thickness between devices further highlights the need for integrated controls in biofilm experiments for reliable evaluation and comparison of new treatments.

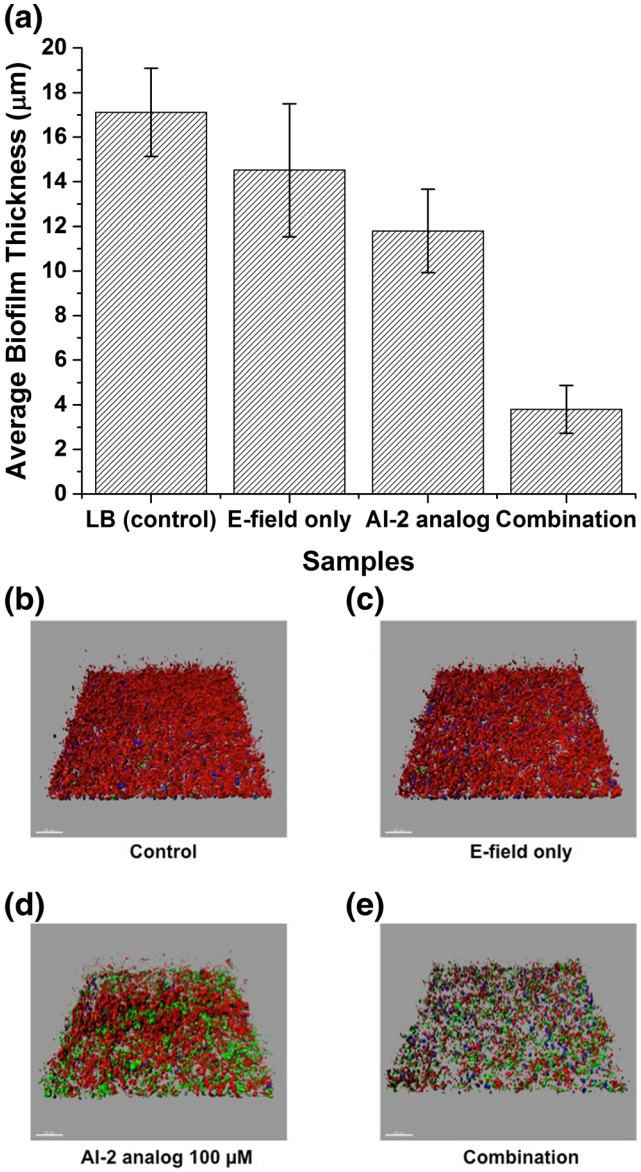

Fig. 7 **a** Average biofilm thickness as measured using the end-point confocal microscopy technique. The combination treatment of AI-2 analogs and electric fields results in a 77.8 ± 6.3 % decrease in biofilm thickness as compared to the control. The error bars represent the standard deviation across three confocal images (n = 3) obtained in each channel of the device. **b**-**e** Surface rendered sample confocal microscopy images from the device (scale bar =20 μm). The thicknesses were 16.87 μm (control), 13.05 μm (E-field only), 10.51 μm (AI-2 analog) and 3.26 μm (combination). The colors in the image correspond to different components of the biofilm. The green and red represents live and dead cells and the blue represents the ECM of the biofilm

3.2.4 Antibiotic-free combination treatment testing using real-time biofilm monitoring

Figure 8 depicts the change in OD during the growth and treatment of *E. coli* biofilms. The high change in OD during the first few hours (from 0 to 3 h) of growth is due to the seeding of the bacterial suspension. The OD then gradually

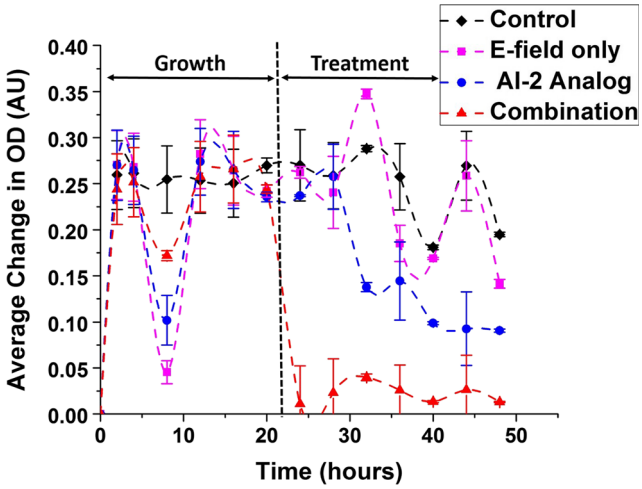

Fig. 8 Measured average change in OD across the length of each channel (n = 186) at representative time points during biofilm growth and treatment. The error bars represent the spatial variance of the biofilm in each of the channels of the device. The variation in OD across the four channels was observed to reduce to 8.5 % (ANOVA, $p < 0.0001$) at the end of the growth period. The channel treated with AI-2 analog and electric fields shows the most significant decrease in biomass

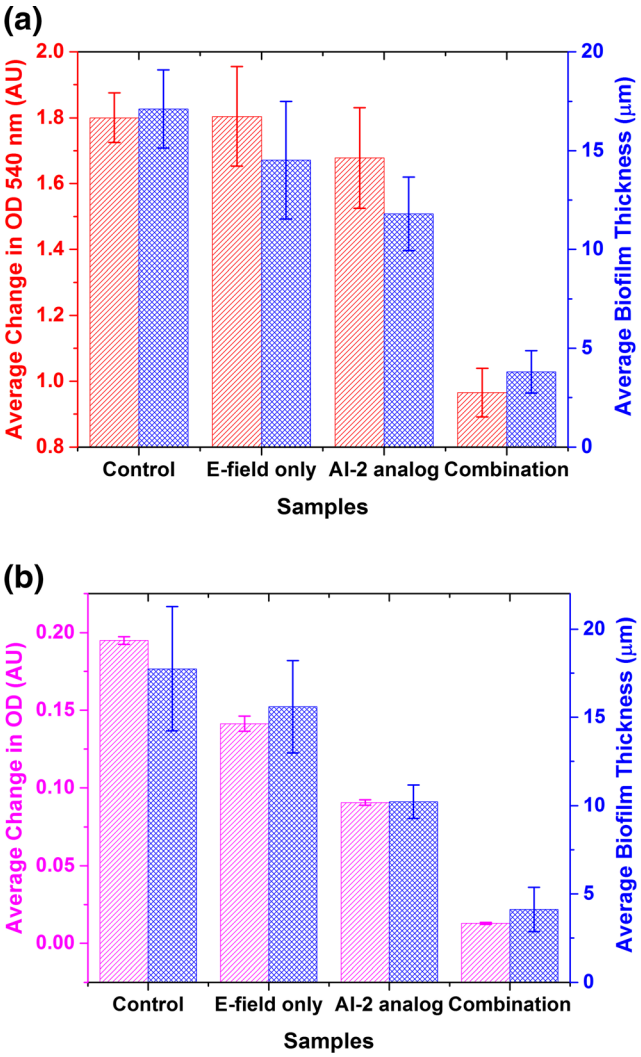

Fig. 9 **a** Measured OD540 after 24 h treatment using the CV staining method and average biofilm thickness (n = 3) measured using end-point confocal microscopy measurements. **b** Measured average change in OD (n = 186) as measured using the CCD platform and average biofilm thickness (n = 2) measured using end-point confocal microscopy after 24 h of treatment

decreased as pure LB media was pumped through the channels (from 3 to 8 h). Following this, small variations in OD observed during hours 10 to 22 were due to biofilm growth and removal. We hypothesize that this is a result of the self-leveling effect experienced by thick biofilms possibly due to the increased shear observed in the microfluidic channel. Statistical correlation between the biomass in the four channels after the growth phase, as measured using the OD measurement setup was demonstrated (ANOVA $p < 0.0001$), thus validating the growth of uniform biofilms in the channels of the device. After 22 h of growth, the variation in biomass was observed to be 8.5 % as compared to the 68 % that was previously measured in single channel microfluidics (Meyer et al. 2011). This reduced biomass variance at the end of the biofilm growth period enables reliable comparison of the various treatments: LB, AI-2 analog, electric fields and a combination of the AI-2 analog and electric fields. Treatment with electric fields-only (pink line) resulted in high correlation in total biomass to the untreated control (black line), whereas AI-2 analog only treatment (blue line) showed a decrease in the biomass with time. The combination treatment (red line) resulted in the most significant decrease in biomass as compared to the control. This correlates well with the end point results obtained using both the CV assay and confocal microscopy.

Figure 9 highlights this correlation between the end-point OD measurements obtained using the macro-scale cuvette setup and the microfluidic CCD setup and the end-point biofilm thicknesses obtained using confocal microscopy. Figure 9a plots the correlation of the macro-scale CV results and the biofilm thicknesses obtained using confocal microscopy for the various treatments applied using the microfluidic bifurcation platform. As observed, small changes in biomass were not detected with high sensitivity using the CV staining method, although the larger changes are easily measured. Due to the inherent lack in sensitivity of the CV staining method, the high resolution confocal measurements obtained using the microfluidic device do not show a very high correlation with the macro-scale measurement ($R^2 = 0.929$). However, as observed from Fig. 9b the correlation between the end-point measurements obtained using the CCD setup and the end-point confocal microscope are statistically significant ($R^2 = 0.980$). This, along with the relative ease of integrating real-time sensors into the microfluidic platform makes microfluidics a better choice for biofilm studies. Even though the CCD set up cannot accurately measure very thin biofilms (<5 μm), the good correlation between the results obtained in

the microfluidic device and the confocal microscopy data, combined with the low variability feature of the bifurcation design, highlight the suitability of our platform for rapid, highly paralleled *in vitro* characterization of novel biofilm treatment strategies.

4 Conclusions

In vivo bacterial biofilm infection eradication using purely antibiotic-based therapies is rendered impossible due to adverse side effects associated with high doses of antibiotics required. In this work we present a novel antibiotic-free treatment for removal of biofilm infections. Our results demonstrate the increased efficacy of a combination therapy using AI-2 analogs and electric fields that is completely independent of traditional antibiotics; the analogs themselves target bacterial cell-cell communication, not viability. This new treatment was tested and verified using both macro-scale and micro-scale test platforms. The macro-scale cuvette setup allowed for measurement of treatment efficacy in a static no-flow environment. The bifurcation-based microfluidic test platform allows for streamlined parallel experiments, using minimal amounts of reagents, while ensuring tighter controls. This design avoids the use of complex structures like microfluidic valves and requires only one step to fabricate making it more amenable to scale-up and integration with other technologies. By integrating a real-time OD measurement system with the microfluidic device, we demonstrate that the combination of AI-2 analogs and electric fields results in a significant decrease in biofilm thickness. We further confirm these results by performing end-point confocal imaging. Treatment with the combination therapy resulted in a significant biofilm thickness decrease of 77.8 % as compared to the untreated controls. We suggest that the increase in treatment efficacy of the AI-2 analog when combined with electric fields is due to the increased permeation of the analog into the bulk of the biofilm. It is also hypothesized that the efficacy of the treatment when using a microfluidic device is greater due to the replenishment of the AI-2 analog molecules at the site of biofilm formation due to continuous flow in the device. Importantly, this finding suggests that this method is promising as a potential treatment and prevention against antibiotic-resistant biofilm infection formation in both the clinical and environmental settings. In the future we envision the use of this treatment for autonomous treatment and removal of biofilm infections on medical implants such as urinary tract catheters and artificial joints, and on environmental biofilms such as those found in water pipes.

Acknowledgments The authors would like to acknowledge the Robert W. Deutsch Foundation, the Centers of Excellence in Regulatory Science and Innovation (CERSI) at the Food and Drug Administration (FDA) and NSF (CBET 1264509) for their financial support. The authors would also like to thank the Maryland Nanocenter and its FabLab staff. Finally, the authors thank Drs. Young Wook Kim and Mariana Meyer for their useful consulting on biofilm growth experiments.

References

S. Al-Nasiry, N. Geusens, M. Hanssens, C. Luyten, R. Pijnenborg, The use of alamar blue assay for quantitative analysis of viability, migration and invasion of choriocarcinoma cells. Hum Reprod (Oxford, England) **22**(5), 1304–1309 (2007)

G.G. Anderson and G.A. O'toole. Innate and Induced Resistance Mechanisms of Bacterial Biofilms. Bacterial Biofilms, Springer**:** 85–105 (2008)

S. A. Blenkinsopp, A. Khoury, J. Costerton, Electrical enhancement of biocide efficacy against pseudomonas aeruginosa biofilms. Appl. Environ. Microbiol. **58**(11), 3770–3773 (1992)

R. Caubet, F. Pedarros-Caubet, M. Chu, E. Freye, M. de Belem Rodrigues, J. Moreau, W. Ellison, A radio frequency electric current enhances antibiotic efficacy against bacterial biofilms. Antimicrob. Agents Chemother. **48**(12), 4662–4664 (2004)

W. Characklis, Bioengineering report: fouling biofilm development: a process analysis. Biotechnol. Bioeng. **23**(9), 1923–1960 (1981)

J. W. Costerton, B. Ellis, K. Lam, F. Johnson, A. E. Khoury, Mechanism of Electrical Enhancement of Efficacy of Antibiotics in Killing Biofilm Bacteria. Antimicrob Agents Chemother **38**(12), 2803–2809 (1994)

J. W. Costerton, P. S. Stewart, E. P. Greenberg, Bacterial biofilms: A common cause of persistent infections. Science **284**(5418), 1318–1322 (1999)

M. P. DeLisa, J. J. Valdes, W. E. Bentley, Mapping stress-induced changes in autoinducer Ai-2 production in Chemostat-cultivated *Escherichia coli* K-12. J. Bacteriol. **183**(9), 2918–2928 (2001)

C. A. Fux, P. Stoodley, L. Hall-Stoodley, J. W. Costerton, Bacterial biofilms: A diagnostic and therapeutic challenge. Expert Rev Anti-Infect Ther **1**(4), 667–683 (2003)

S. Gamby, V. Roy, M. Guo, J. A. Smith, J. Wang, J. E. Stewart, X. Wang, W. E. Bentley, H. O. Sintim, Altering the communication networks of multispecies microbial systems using a diverse toolbox of Ai-2 analogues. ACS Chem. Biol. **7**(6), 1023–1030 (2012)

M. Ghannoum and G.A. O'Toole. Microbial Biofilms, ASM Press (2004)

M. Giladi, Y. Porat, A. Blatt, E. Shmueli, Y. Wasserman, E. D. Kirson, Y. Palti, Microbial growth inhibition by alternating electric fields in mice with pseudomonas aeruginosa lung infection. Antimicrob. Agents Chemother. **54**(8), 3212–3218 (2010)

A. Heydorn, A. T. Nielsen, M. Hentzer, C. Sternberg, M. Givskov, B. K. Ersbøll, S. Molin, Quantification of biofilm structures by the novel computer program Comstat. Microbiology **146**(10), 2395–2407 (2000)

A. Huq, C. A. Whitehouse, C. J. Grim, M. Alam, R. R. Colwell, Biofilms in water, its role and impact in human disease transmission." current opinion in. Biotechnology **19**(3), 244–247 (2008)

W. Jun, M. S. Kim, B.-K. Cho, P. D. Millner, K. Chao, D. E. Chan, Microbial biofilm detection on food contact surfaces by macro-scale fluorescence imaging. J. Food Eng. **99**(3), 314–322 (2010)

Y.W. Kim, M.P. Mosteller, M.T. Meyer, H. Ben-Yoav, W.E. Bentley and R. Ghodssi. Microfluidic biofilm observation, analysis, and treatment (Micro-Boat) Platform. Hilton Head Workshop 2012: A solid-state sensors, actuators and microsystems workshop, Hilton Head, SC (2012)

Y. W. Kim, S. Subramanian, K. Gerasopoulos, H. Ben-Yoav, H.-C. Wu, D. Quan, K. Carter, M. T. Meyer, W. E. Bentley, R. Ghodssi, Effect

of electrical energy on the efficacy of biofilm treatment using the bioelectric effect. Npj Biofilms Microbiomes **1**, 15016 (2015)

Y. W. Kim, M. P. Mosteller, S. Subramanian, M. T. Meyer, W. E. Bentley, R. Ghodssi, An optical microfluidic platform for spatiotemporal biofilm treatment monitoring. J Micromech Microeng **26**(1), 015013 (2016)

J.H. Merritt, D.E. Kadouri and G.A. O'Toole. Growing and analyzing static biofilms. Current protocols in microbiology, John Wiley & Sons, Inc. (2005)

M. T. Meyer, V. Roy, W. E. Bentley, R. Ghodssi, Development and validation of a microfluidic reactor for biofilm monitoring via optical methods. J Micromech Microeng **21**(5), 054023 (2011)

M. T. Meyer, S. Subramanian, Y. W. Kim, H. Ben-Yoav, M. Gnerlich, W. E. Bentley, R. Ghodssi, Multi-depth Valved microfluidics for biofilm segmentation. J. icromech. Microeng. **25**, 095003 (2015)

M. B. Miller, B. L. Bassler, Quorum sensing in bacteria." annual reviews in. Microbiology **55**(1), 165–199 (2001)

G.A. O'Toole, L.A. Pratt, P.I. Watnick, D.K. Newman, V.B. Weaver and R. Kolter. Genetic approaches to study of biofilms. Methods in Enzymology. J.R. Doyle, Academic Press. 310**:** 91–109 (1999).

A. Pareilleux, N. Sicard, Lethal effects of electric current on *Escherichia coli*. Appl Microbiol **19**(3), 421–424 (1970)

J. Pozo, R. Patel, The challenge of treating biofilm-associated bacterial infections. Clin Pharmacol Ther **82**(2), 204–209 (2007)

D. N. Quan, W. E. Bentley, Gene network homology in prokaryotes using a similarity search approach: queries of quorum sensing signal transduction. PLoS Comput Biol **8**(8), e1002637 (2012)

T. B. Rasmussen, M. Givskov, Quorum sensing inhibitors: a bargain of effects. Microbiology **152**(4), 895–904 (2006a)

T. B. Rasmussen, M. Givskov, Quorum-sensing inhibitors as anti-pathogenic drugs. International Journal of Medical Microbiology **296**(2–3), 149–161 (2006b)

B. W. Roberts, W. L. Olbricht, The distribution of freely suspended particles at microfluidic bifurcations. AICHE J. **52**(1), 199–206 (2006)

V. Roy, R. Fernandes, C.-Y. Tsao, W. E. Bentley, Cross species quorum quenching using a native Ai-2 processing enzyme. ACS Chem. Biol. **5**(2), 223–232 (2009)

V. Roy, J. A. Smith, J. Wang, J. E. Stewart, W. E. Bentley, H. O. Sintim, Synthetic analogs tailor native Ai-2 signaling across bacterial species. J. Am. Chem. Soc. **132**(32), 11141–11150 (2010)

V. Roy, B. L. Adams, W. E. Bentley, Developing next generation antimicrobials by intercepting ai-2 mediated quorum sensing. Enzym Microb Technol **49**(2), 113–123 (2011)

V. Roy, M. T. Meyer, J. A. I. Smith, S. Gamby, H. O. Sintim, R. Ghodssi, W. E. Bentley, Ai-2 analogs and antibiotics: a synergistic approach to reduce bacterial biofilms. Appl. Microbiol. Biotechnol. **97**(6), 2627–2638 (2013)

P. S. Stewart, W. Wattanakaroon, L. Goodrum, S. M. Fortun, B. R. McLeod, Electrolytic generation of oxygen partially explains electrical enhancement of tobramycin efficacy against pseudomonas aeruginosa biofilm. Antimicrob. Agents Chemother. **43**(2), 292–296 (1999)

P. Stoodley, D. DeBeer, H. M. Lappin-Scott, Influence of electric fields and Ph on biofilm structure as related to the bioelectric effect. Antimicrob. Agents Chemother. **41**(9), 1876–1879 (1997)

P. Stoodley, K. Sauer, D. Davies, J. W. Costerton, Biofilms as complex differentiated communities. annual reviews in. Microbiology **56**(1), 187–209 (2002)

S. Subramanian, Y.W. Kim, M.T. Meyer, H.O. Sintim, W.E. Bentley and R. Ghodssi. A real-time bacterial biofilm characterization platform using a microfluidic system. Hilton Head Workshop 2014: A solid-state sensors, actuators and microsystems workshop, Hilton Head, SC (2014)

S. Subramanian, K. Gerasopoulos, H.O. Sintim, W.E. Bentley and R. Ghodssi. A bacterial biofilm combination treatment using a real-time microfluidic platform. The 18th international conference on solid-state sensors, actuators and microsystems (Transducers), Anchorage, AK (2015)

K. Toté, D. V. Berghe, L. Maes, P. Cos, A new colorimetric microtitre model for the detection of *Staphylococcus aureus* biofilms. Lett. Appl. Microbiol. **46**(2), 249–254 (2008)

L. Wang, J. Li, J. C. March, J. J. Valdes, W. E. Bentley, Luxs-dependent Gene regulation in *Escherichia coli* K-12 revealed by genomic expression profiling. J. Bacteriol. **187**(24), 8350–8360 (2005)

C. M. Waters, B. L. Bassler, Quorum sensing: cell-to-cell communication in bacteria. Annu. Rev. Cell Dev. Biol. **21**, 319–346 (2005)

N. Wellman, S. M. Fortun, B. R. McLeod, Bacterial biofilms and the bioelectric effect. Antimicrob. Agents Chemother. **40**(9), 2012–2014 (1996)